Received 30 November 2023; Accepted 13 February 2024
https://doi.org/10.48612/letters/2024-1-79-84

Phase-field modeling of changes in the grain structure of 316L steel obtained by cold spraying followed by laser treatment

M. S. Orlova†, A. I. Gorunov

†oms1999@yandex.ru

Kazan National Research Technical University n. a. A. N. Tupolev — KAI, Kazan 420111, Russia

Abstract: The work is devoted to the study of the grain structure of alloy 316L, obtained by supersonic laser deposition. The purpose of this paper is to study the formation of the grain structure of the metal obtained by cold spraying method and treated by laser. Recrystallization processes are simulated using the phase field method. The effect of a concentrated energy source on the grain structure of the metal was described by the non-stationary Allen-Kahn and Kahn-Hilliard equations. The simulation results showed that during the thermal action of the laser, the grains diffused and increased in size. The regularity of grain growth in the direction of the current temperature gradient was also found. The simulation results were confirmed by the results of several experiments conducted to verify them.

Keywords: cold spraying, laser radiation, mathematical modeling, phase field method

1. Introduction

Currently, the method of cold spraying is one of the simplest and most effective methods of coating. Cold spraying allows one to preserve the mechanical properties and chemical composition of the initial powder material to a greater extent. Using the cold spraying method, it is possible to create products that are superior in their properties to coatings applied using a laser source, which expands the use of cold spraying for additive manufacturing [1, 2]. However, in the case of using refractory materials as feedstock or incorrect selection of process parameters, as a result, coating stratification may occur, which happens due to insufficient adhesion of powder particles [3].

The microstructure of a coating obtained by cold spraying is a collection of particles of the source material bonded at the edges with each other due to strong kinetic action. Structures of this type do not always have sufficiently good strength indicators, so in some cases laser exposure is used in addition to cold spraying. Laser radiation treatment has a positive effect on the hardness index of the resulting coating, as well as on the density of the resulting coating due to recrystallization processes [4 – 6]. The addition of laser exposure to the cold spraying process makes it possible to control the structure of the resulting coatings and allows you to obtain materials with a gradient structure.

In the supersonic laser deposition (SLD) technology, the laser beam acts on the substrate directly during the cold spraying process [7, 8]. This method of application makes it possible to obtain more homogeneous non-porous coatings due to the heating of the substrate and the flow of deposited particles near the substrate. By the SLD method, it is possible to obtain better adhesion due to plastic deformation of particles, while using lower deposition rates than with cold spraying [9 –12].

Laser exposure can also be performed as a post-treatment of coatings obtained by various methods of supersonic spraying, in the form of laser remelting of the finished coating [13,14]. Additional laser exposure to the sprayed coating makes it denser, and also significantly increases its microhardness and adhesive strength.

However, this technology and the processes occurring during laser exposure are still poorly understood, it is almost impossible to trace them directly at the time of the process itself. Therefore, in such cases, the optimal solution is to create a mathematical model of the formation of the metal structure of multilayer coatings obtained by the cold spraying with laser intensification (CSL) method, taking into account all the main factors and processes. Mathematical modeling with a certain accuracy of the model allows us to trace the patterns of changes in the grain structure of the material at various parameters.

2. Model and computational procedure

In the phase field method, the defining equations for modeling the formation of a grain structure are the non-stationary Ginzburg–Landau equations, including the Allen–Cahn and Cahn–Hillard equations [15,16]. Also, in order to simulate the effect of laser radiation on the material, it is necessary to include a non-stationary thermal conductivity equation in the mathematical model of the process.

The Allen–Cahn equation is solved separately for each grain of polycrystalline material. The non-stationary Allen–Cahn equation contains a functional derivative of free energy:

$$\frac{\partial \eta}{\partial t} = -L_{\eta} \frac{\delta F}{\delta \eta}, \qquad (1)$$

where η is the phase field variable, L_{η} is the kinetic coefficient associated with the interphase mobility of the interface

between the liquid and solid phases, F is the free energy functional (2). According to [17], the free energy functional can be described as follows:

$$F = \int_V \left(f_{\text{chem}} + f_{\text{doub}} + f_{\text{grad}} \right) dV, \tag{2}$$

where f_{chem} is the density of free chemical energy, which is an interpolation of free energies in the solid phase f_S and liquid f_L with a monotonically increasing function $p(\eta)$ (Eq. 3), f_{doub} is a potential with two minimums corresponding to the equilibrium points of the existence of solid and liquid phases, taking into account the energy barrier height W at the interface of the solid phase and liquid (Eq. 4), f_{grad} is the gradient energy density with the energy gradient coefficient for a parameter of the order k_η (Eq. 5).

$$f_{\text{chem}} = p(\eta) f_S + (1 - p(\eta)) f_L, \text{ at } p(\eta) = \eta^3(10 - 15\eta + 6\eta^2) \tag{3}$$

$$f_{\text{doub}} = Wq(\eta), \text{ at } q(\eta) = \eta^2(1-\eta)^2 \tag{4}$$

$$f_{\text{grad}} = \frac{k_\eta}{2} \left| \nabla \eta \right|^2. \tag{5}$$

The function q is chosen in such a way that it takes the maximum value at the phase interface ($\eta = 0.5$) and is zero in the solid and liquid phases. Substituting expressions (3 – 5) into the equation for free energy (2), we can obtain the following expression for the functional derivative:

$$\begin{aligned} &\frac{\partial f_{\text{chem}}}{\partial \eta} + \frac{\partial f_{\text{doub}}}{\partial \eta} - \nabla \cdot \frac{\partial f_{\text{grad}}}{\partial (\nabla \eta)} = \\ &\quad = 30\eta^2 + 2W\eta(1-\eta)(1-2\eta) - k_\eta \nabla^2 \eta. \end{aligned} \tag{6}$$

Then, when substituting expression (6), the Allen–Kahn equation (1) is written as follows:

$$\frac{\partial \eta}{\partial t} = L_\eta \left(4W\eta(1-\eta)\left(\eta - \frac{1}{2} + \frac{15}{2W}\eta(1-\eta)(f_L - f_S) \right) + k_\eta \nabla^2 \eta \right). \tag{7}$$

The expression $(f_L - f_S)$ is written as a thermodynamic driving force:

$$f_L - f_S = \frac{L_m (T_m - T)}{T_m}, \tag{8}$$

where L_m is the latent heat of melting, T_m is the melting point, T is the current temperature.

The non-stationary thermal conductivity equation describing the dynamics of heating of a material by a laser source Q can be written as:

$$\rho C_p \frac{\partial T}{\partial t} = k \nabla^2 T + Q, \tag{9}$$

where ρ is the density of the material, C_p is the heat capacity of the material, k is the thermal conductivity coefficient of the material, Q is the volumetric heat source.

The Kahn–Hillard equation determines the change in the concentration of material c during the formation of the grain structure of the metal:

$$\frac{\partial c}{\partial t} = \nabla \left(D \nabla \frac{\delta F}{\delta c} \right), \tag{10}$$

where D is the diffusion coefficient.

The diffusion coefficient consists of four components [18,19]: volume diffusion, surface diffusion, grain boundary diffusion and evaporation diffusion (Eq. 11), their action is schematically depicted in Fig. 1.

$$\begin{aligned} D = {} & D_{\text{vol}} p_{\text{vol}}(c) + D_{\text{surf}} c(1-c) + \\ & + D_{\text{GB}} \sum_i \sum_{i \neq m} \eta_i \eta_m + D_{\text{vap}} \left(1 - p_{\text{vol}}(c)\right), \end{aligned} \tag{11}$$

where D_{vol}, D_{surf}, D_{GB}, D_{vap} are the coefficients of the corresponding diffusions, $p_{\text{vol}}(c)$ is the boundary interpolation function $p_{\text{vol}}(c) = c^3(10 + 15c + 6c^2)$. It is taken into account that recrystallization occurs not only inside the particles, but also at the boundaries between the particles, which helps improve the interaction between particle boundaries due to the atomic diffusion of atoms [20].

To further solve the equations, their discretization was performed using the finite difference method. For the two-dimensional case with the same grid step $\Delta x = \Delta y = h$, the Allen–Kahn equation (7) is written implicitly as:

$$\begin{aligned} &\frac{\eta_{ij}^{k+1} - \eta_{ij}^k}{\tau} = \\ &= L_\eta \left(\begin{array}{c} k_\eta \dfrac{\eta_{i+1j}^k + \eta_{i-1j}^k + \eta_{ij+1}^k + \eta_{ij-1}^k - 4\eta_{ij}^k}{h^2} + 4W\eta_{ij}^k \\ \left(1 - \eta_{ij}^k\right)\left(\eta_{ij}^k - \dfrac{1}{2} + \dfrac{15}{2W}\eta_{ij}^k \left(1 - \eta_{ij}^k\right)\left(\dfrac{L_m \left(T_m - T_{ij}^k\right)}{T_m} \right) \right) \end{array} \right), \end{aligned} \tag{12}$$

where τ is a time step, h is a spatial step.

Thermal conductivity equation (9) in finite difference form:

$$\begin{aligned} &\rho C_p \frac{T_{ij}^{k+1} - T_{ij}^k}{\tau} = \\ &\quad = k \frac{T_{i+1j}^k + T_{i-1j}^k + T_{ij+1}^k + T_{ij-1}^k - 4T_{ij}^k}{h^2} + \frac{W_Q}{h\pi r^2}. \end{aligned} \tag{13}$$

The Kahn–Hillard equation (10) in finite difference form:

$$\begin{aligned} &\frac{c_{ij}^{k+1} - c_{ij}^k}{\tau} = \\ &\quad = D \left(\frac{\varsigma_{i+1j}^k + \varsigma_{i-1j}^k + \varsigma_{ij+1}^k + \varsigma_{ij-1}^k - 4\varsigma_{ij}^k}{h^2} \right), \end{aligned} \tag{14}$$

where ς_{ij}^k is written as:

$$\begin{aligned} \varsigma_{ij}^k = {} & 2c_{ij}^k + 4\sum_{i=1}^{p} \eta_i^3 - 6\sum_{i=1}^{p} \eta_i^2 - 32c_{ij}^k \left(1 - c_{ij}^k\right)^2 + \\ & + 32{c_{ij}^k}^2 \left(1 - c_{ij}^k\right) - k_c \frac{c_{i+1j}^k + c_{i-1j}^k + c_{ij+1}^k + c_{ij-1}^k - 4c_{ij}^k}{h^2}. \end{aligned} \tag{15}$$

To simulate the process of forming a grain structure, stainless steel of the austenitic class 316L was selected as the material. The model was implemented in the MATLAB software environment in two different projections. As an initial picture of the distribution of the grain structure, a fine-grained structure consisting of equiaxed crystals was chosen, which is shown in Fig. 2. This microstructure corresponds to the material obtained by cold spraying, when each powder particle forms one crystal.

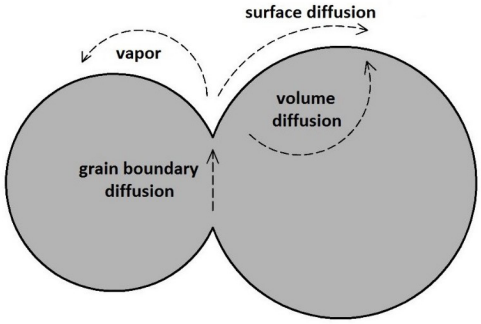

Fig. 1. Diagram of the action of diffusion processes.

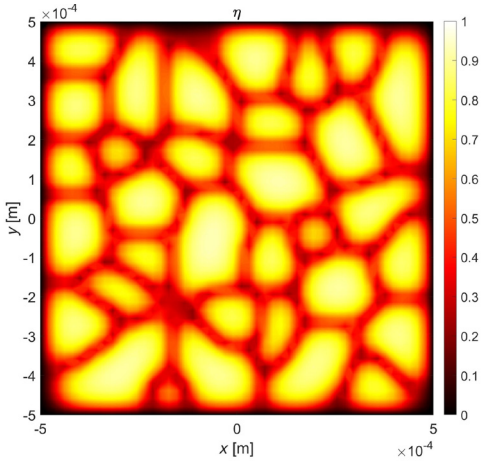

Fig. 2. (Color online) Initial distribution of the grain structure.

3. Materials and experimental methods

To obtain multilayer coatings made of stainless steel, a CSL unit was used. During the CSL process, a jet of powder mixture exits the nozzle and is directed towards the substrate. The powder particles hit the substrate surface when simultaneously exposed to a fiber laser beam with a wavelength of 1070 nm and a maximum power of 6 kW.

The process of applying the multilayer coating was carried out at a constant temperature controlled by a pyrometer, and the laser power is periodically set by an automatic control system built into the software. The supersonic nozzle, laser head and pyrometer were stationary in the process, and all moving parts are controlled by a robot. To apply the multilayer coating, spherical powder particles made of 316L alloy with an average diameter of 10 – 50 micrometers were used. A laser power of 2 kW was used to melt the surface of multilayer coatings with a laser. A total of 10 layers of 316L coating were deposited. The laser exposure occurred at a depth of one layer, about 200 – 250 micrometers.

The surface structure of the metallographic sample was analyzed using an Auriga CrossBeam electron microscope and a Tescan Mira 3 electron microscope (FESEM) equipped with an electron backscattering diffraction (EBSD) detector.

4. Results and discussion

Figure 3 shows laser-treated multilayer coatings made of 316L steel obtained by the CSL method. Laser surface treatment

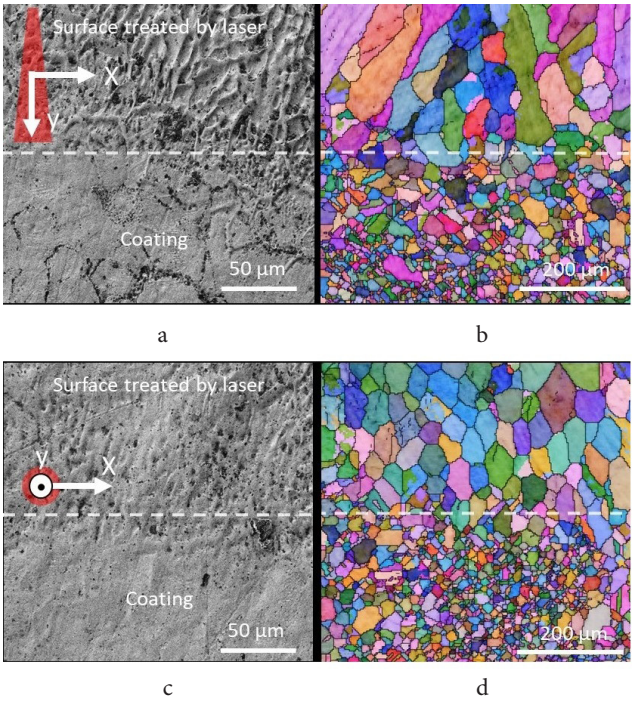

Fig. 3. (Color online) SEM and EBSD images of the sample in the orientation of the laser beam in a section parallel (a, b) and perpendicular (c, d) to the laser beam.

made it possible to obtain a directional structure in the surface layers. When examining the laser-treated surface of the CSL coating using a scanning electron microscope, the direction of grain growth is observed (Fig. 3 a, c). As a result of crystallization, columnar grains were formed, directed towards the action of the heat source, which was a laser beam.

The data obtained by the EBSD method give an idea of the diameter and orientation of austenitic grains (Fig. 3 b, d). Figure 3 b shows that the grains are elongated in the direction corresponding to the action of a heat source in the form of a laser beam and are directed mainly in the direction of the Y coordinate. The average grain size is 300 – 500 micrometers for a section of the sample treated with a laser in the direction parallel to the laser beam (longitudinal section) (Fig. 3 a, b), the average grain size is 70 – 100 micrometers for a section in the sample in the direction perpendicular to the laser beam (vertical cross section) (Fig. 3 c, d).

At the same time, the data of the EBSD analysis show that each particle of the 316L powder that makes up the CSL coating consists of small grains. In the cross section perpendicular to the movement of the laser beam, the average diameter of the coating grain not treated with a laser is 10 – 70 micrometers. There is a known tendency for directed growth of metal grains under the action of a significant temperature gradient. This statement is also applicable for processing material with concentrated energy sources.

Zhang et al. [9] showed that in the process of complete laser melting, the directed growth of columnar grains occurs in the direction of the thermal center. At the same time, the grain size of the metal obtained using laser cladding and supersonic laser deposition technology is 10 times larger respectfully, which confirms the results of experimental studies obtained in our study.

Next, the results of mathematical modeling of the process will be considered. Figures 4 – 5 show the process of forming a grain structure in a vertical cross section at various points in time in the form of a graphical representation of four parameters: radiation source ($Spot_{heated}$), temperature field (T), phase field (η) and concentration (c). At the initial moment of the process, a molten pool is formed in the left side of the calculation area. After that, as the laser moves, the temperature front shifts to the right boundary of the region. Yang et al. [15] investigated the shape of the melt bath and confirmed the possibility of the formation of zones of thermal influence of the metal processed by the laser. Thus, it can be assumed that a subgrain structure may appear at the boundary between the processed layer and the substrate.

During the crystallization of the molten pool, columnar grains are formed, elongated in the direction of movement of the laser source. The phenomenon of the formation of a zone of columnar crystals is explained by the fact that in the center part of the molten pool, the cooling of the material was the slowest, that is, the greatest temperature gradient was observed. Cusato et al. [16] confirmed by mathematical modeling that the change in the thermal center during laser treatment of the metal surface sets the direction for grains and dendritic crystals, thus a detailed mathematical model made it possible to predict with high accuracy the orientation and average size of the structural components of the metal based on analysis and comparison with experimental data. There is a process of enlargement of grains located in the heat trace zone, but not subjected to melting. This phenomenon is associated with the processes of grain boundary diffusion, which increases with increasing temperature. A similar phenomenon is observed in the EBSD images shown above.

After the end of the laser action on the material and its complete cooling below the melting point, the final result of the formation of a grain structure in a vertical cross section can be observed. The time of complete crystallization of the melt was approximately 15 ms.

Figures 6 – 7 show the process of changing the grain structure during the movement of the laser source in the longitudinal section. At the initial moment of the laser source action on the material, a molten pool is formed. Further along the course of the laser source movement, the temperature

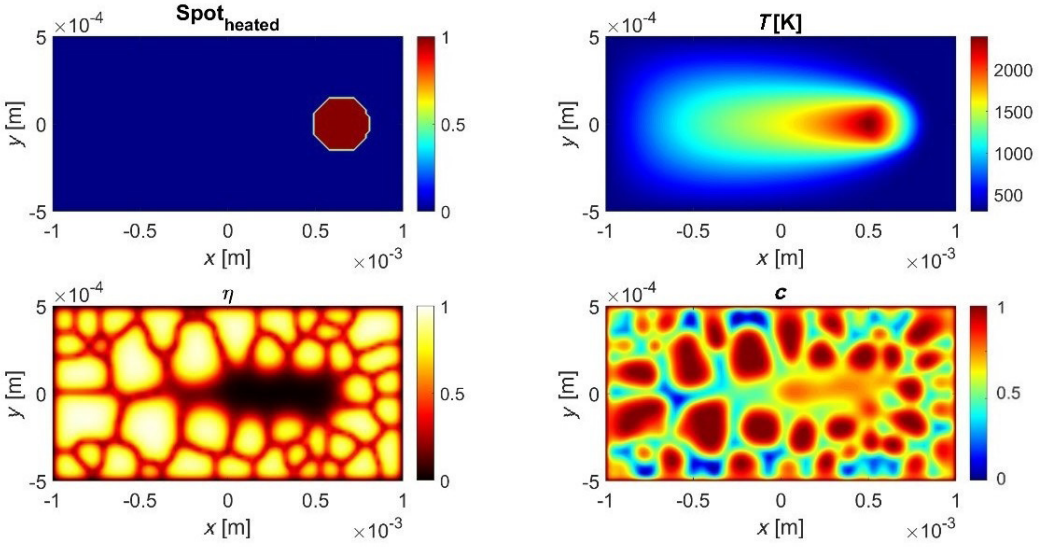

Fig. 4. (Color online) The result of modeling changes in the microstructure during the movement of a laser source at a time of 10.3 ms.

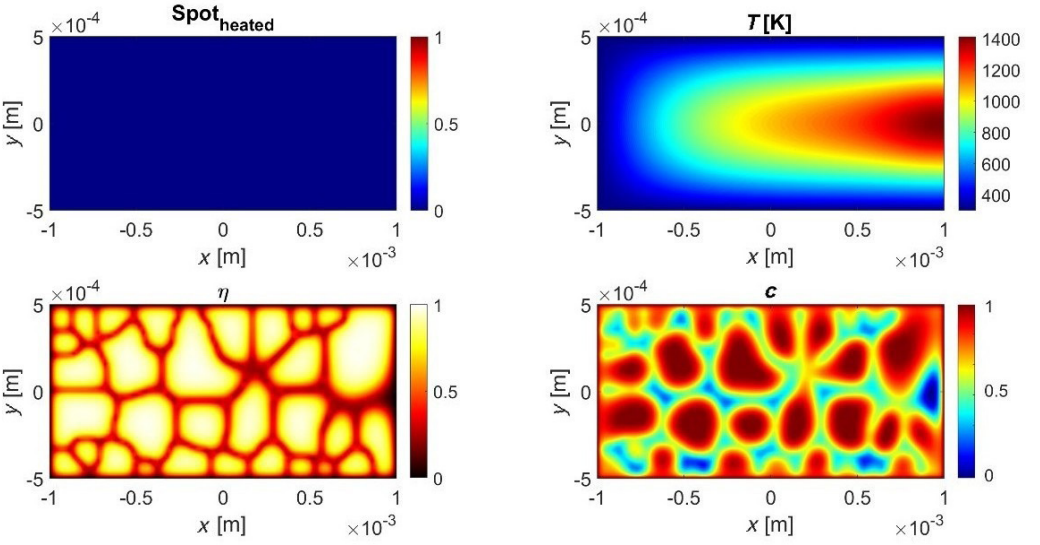

Fig. 5. (Color online) The result of modeling changes in the microstructure during the movement of a laser source at a time of 18.8 ms.

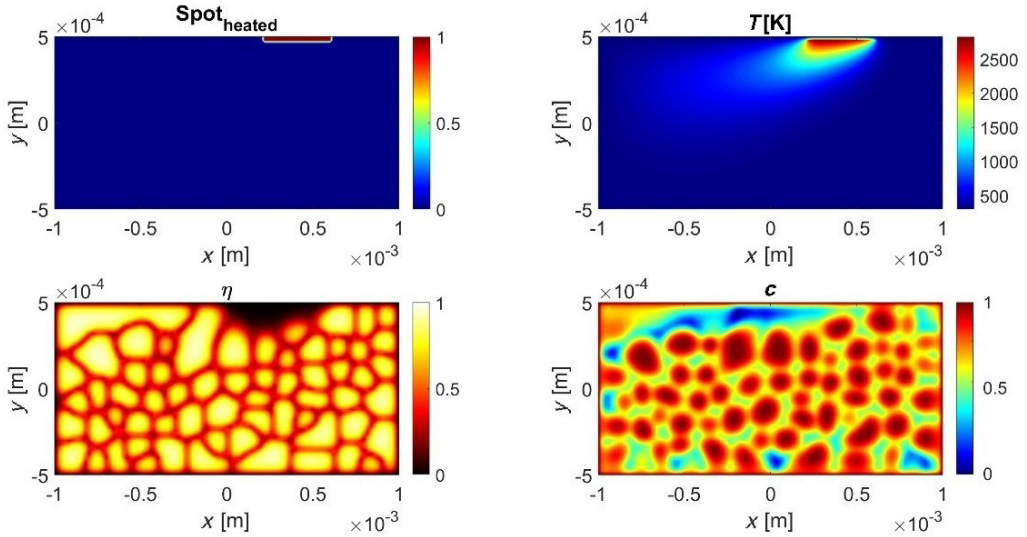

Fig. 6. (Color online) The result of modeling changes in the microstructure during the movement of a laser source at a time of 11.1 ms.

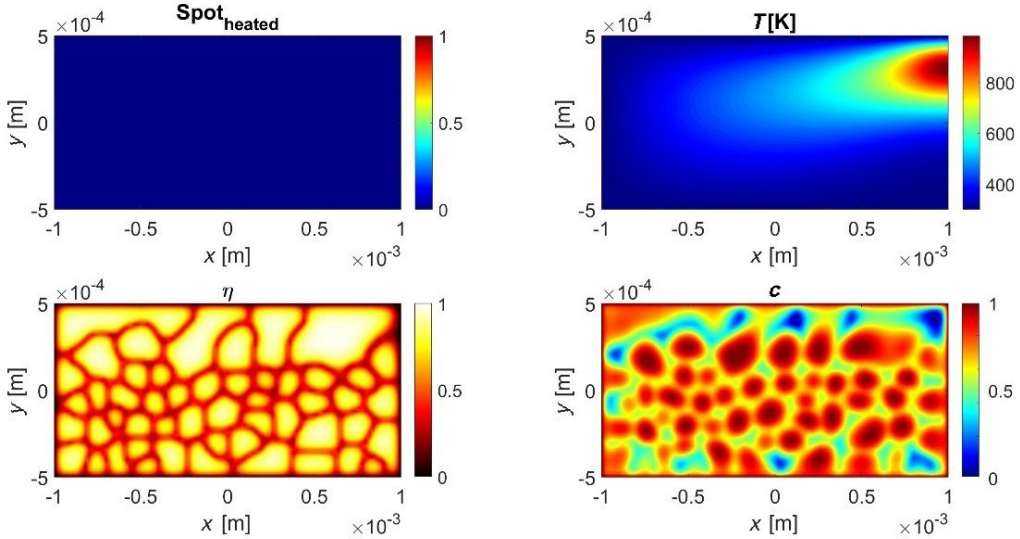

Fig. 7. (Color online) The result of modeling changes in the microstructure during the movement of a laser source at a time of 17.3 ms.

front changes. Behind the molten pool, grains are formed, elongated in the direction of the laser movement.

The time of complete crystallization of the melt was approximately 15 ms. As a result of laser exposure, the grains of the surface layer were enlarged. At the same time, a fine-grained structure has been preserved in the zone of the source material.

A similar growth of columnar metal grains elongated in the direction of the temperature gradient when exposed to laser radiation was demonstrated by Javed et al. [21], where the crystallization process was modeled using the cellular automata method. Yao et al. [22] also obtained similar results of modeling changes in the grain structure of a metal by the phase field method.

According to the results of the research, the calculation of the grain elongation coefficient obtained and calculated using the model during laser radiation treatment was carried out. The grain elongation coefficient was calculated as the ratio of the average grain size after laser treatment to the average grain size before treatment. The calculation results are shown in Table 1.

Table 1. The obtained and calculated grain elongation coefficient.

Longitudinal section		Vertical cross section	
Obtained	Calculated	Obtained	Calculated
5.22	4.35	3.81	3.36

Within the accepted assumptions and boundary conditions of the mathematical model, the calculated values are comparable to the results of the real CSL process.

5. Conclusions

In the present research, a mathematical model of the evolution of the grain structure of 316L steel manufactured by CSL was developed and implemented. Mathematical modeling of steel processing by laser radiation in two different projections is carried out. The results of modeling changes in the grain structure were found to be accurate and reliable due to comparison with experimental results. After exposure to laser radiation, the effect of enlargement and elongation of the grains in the direction of the action of the

heat source was observed. Grain elongation coefficients were calculated for the structure obtained and calculated using the model in two projections. The coefficients are close in value, which once again confirms the reliability of the developed mathematical model of the process.

Acknowledgements: *The research was carried out with the financial support of the Russian Science Foundation within the framework of scientific project No. 23-29-00219.*

References

1. W. Li, K. Yang, S. Yin, X. Yang, Y. Xu, R. Lupoi.J. of Mater. Sci. and Tech. 34 (3), 440 (2018).
2. S. Bagherifard, S. Monti, M.V. Zuccoli, M. Riccio, J. Kondas, M. Guagliano. Mater. Sci. and Engin.: A. 721, 339 (2018).
3. Z. Wang, C. Han, H. Guosheng, B.Han.Rapid Prototyping J. 28 (2), 330 (2022).
4. M. Bray, A. Cockburn, W. O'Neill. Surface and Coating Technology. 203 (19), 2851 (2011).
5. B. Li, Z. Li, L. Yang, J. Yao. Paton Weld. J. 8, 35 (2016).
6. S. Wang, L. Cui, G. Liu, J. Hao, X. Wang, E. Hao. Surf. and Coat. Tech. 453, 129142 (2023).
7. A.I. Gorunov. J. of Therm Spray Tech. 27, 1194 (2018).
8. A.I. Gorunov. J. of Manufact. Proc. 56, 746 (2020).
9. Q. Zhang, L. Wu, H. Zou, B. Li, G. Zhang, J. Sun, J. Wang, J. Yao. J. of Alloys and Compounds. 860, 158417 (2021).
10. J.H. Yao, L.J. Yang, B. Li, Z.H. Li. Mater. and Design. 83, 26 (2015).
11. J. Yao, Z. Li, B. Li, L. Yang. J. of Alloys and Compounds. 661, 526 (2016).
12. R. Lupoi, M. Sparkes, A. Cockburn, W. O'Neill. Mater. Letters. 65 (21-22), 3205 (2021).
13. B. Han, S. Bei, G. Han, W. Du, S. Zhu, X. Yan, W. Hang, F. Cui, W. Du, W. Xu, J.Qiu. Optics and Laser Tech. 132 (1–2), 106467 (2020).
14. K. Chong, Y. Zou, D. Wu, Y. Tang, Y. Zhang. Surf. and Coat. Tech. 418, 127258 (2021).
15. M. Yang, L. Wang, W. Yan. Npj Comput. Mater. 7 (1), 56 (2021).
16. N. Cusato, S.A. Nabavizadeh, M. Eshraghi. Metals. 13 (7), 1169 (2023).
17. T. Takaki. ISIJ International. 54 (2), 437 (2014).
18. Y.U. Wang. Acta Mater. 54 (4), 953 (2006).
19. X. Wang, Y. Liu, L. Li, C.O. Yenusah, Y. Xiao, L. Chen. Mater. and Design. 203 (10), 109615 (2021).
20. S. Yin, R. Jenkins, X. Yan, R. Lupoi. Mater. Sci. and Engin.: A. 734, 67 (2018).
21. A. Javed, C. Pradeep, P. Deepankar, S. Brent. Additive Manufacturing. 21, 255 (2021).
22. X.X. Yao, X. Gao, Z. Zhang. Additive Manufacturing. 20, 934 (2022).